Sociedad Mexicana de Ingeniería Mecánica
Fecha de recepción: 13-01-2018
Fecha de aceptación: 25-04-2018

INGENIERÍA MECÁNICA
TECNOLOGÍA Y DESARROLLO
Vol. 6 No. 2 (2018) 053 - 059

Microstural Effects and Large Microhardness in Hypereutectic Al-Fe Alloy Processed by Laser Surface Remelting

Moises Meza Pariona, Katieli Tives Micene
Graduate Program in Engineering and Materials Science,
State University of Ponta Grossa (UEPG), Ponta Grossa 84010-919, PR, Brazil
Correspondent author: Moises Meza Pariona, mmpariona°uepg.br

Resumen

En este trabajo fue utilizado la liga Al-2.0% Fe hipereutectico, toda la superficie de la muestra fue cubierta con files de soldadura consecutivas y superpuestas mediante la técnica de refusión superficial a láser (RSL). En esta superficie tratada fue realizado un análisis micro estructural y bien como pruebas de microdureza. La microestructura fue analizada mediante el microscopio óptico, microscopia de electrónico de barredura de emisión de campo (MEBEC) y por la técnica Vickers. Los resultados obtenidos en este estudio muestran, que por el tratamiento por RSL se produjo un brusco calentamiento localizado y seguido por rápido resfriamiento de la región tratada, resultando así la formación de una capa fina de microestructura, llevando a disolución de precipitados e inclusiones, por consiguiente generando la formación de fases meta estables, aun, desprovisto de micro fisuras en la región fundida y con una protuberancia pequeña en los filetes de la soldadura, resultando así una característica homogénea de la región tratada que el substrato. El análisis de la dureza por Vickers se ha realizado en el área de la sección transversal y en la superficie del cuerpo de prueba. Resultando una alta microdureza en la región tratada que en el substrato no tratado.

Abstract

In this work hypereutectic Al-2.0 wt% Fe alloy was used, the whole surface of the sample was covered with consecutive and superimposed weld fillets by means of laser surface remelting (LSR) technique. Microstructure was analyzed by optical microscopy, field-emission scanning electron microscopy and Vickers technical. Results obtained in this study indicate in LSR-treatment occurred rapid heating and followed by rapid cooling, resulting in formation of a thin recast layer with a refined microstructure, with dissolution of precipitates and inclusions, and formation of metastable phases, devoid of microcracks in the cast region and with smaller protuberance on the weld fillets, resulting so a homogeneous characteristic of the treated region that the substrate. Furthermore, analysis of Vickers hardness was done in the cross-sectional area of treated sample and on the treated sample surface. Resulting in a greater microhardness of the treated region than untreated substrate.

Palabras clave:
Refusión superficial a láser, Al-2,0%Fe, microestructura, microdureza, MO, MEBEC

Keywords:
Laser surface remelting, Al-2.0 wt.% Fe, microstructure, microhardness, OM, FESEM

Introduction

Laser surface remelting (LSR) has attracted increasing interest in recent years due to its special capabilities. High energy density of LSR translates into efficient use of energy for remelting, because LSR modifies surface properties of a material without affecting its bulk properties. LSR results in rapid quenching of the molten material by conduction into the cold subsurface after rapid irradiation. This type of behavior was also observed by Kalita [1], who applied laser surface melting (LSM) technique in a study of high strength aluminum alloys (HSAL).

Pariona et al. [2, 3] used LSR technique in a study of hypoeutectic Al-1.5 wt.% Fe alloy. Characterization of the cast region revealed the formation of a refined, dense and highly homogeneous microstructure, as well as cracking, noticeably with a high formation of protuberance on the weld fillets than alloy untreated. An overlapping line of consecutive weld fillets was also perceptible in the cast region of this alloy, which resulted in an increase of about 61% in hardness compared to the base material. According to Pariona and et al. [4], which the Marangoni effect influence thermal gradient in the molten pool a high temperature, meanwhile, also it produces effects in quality and properties of microstructure, morphological characteristic and as well as quality of laser-treated workpiece track. Yet these same authors confirmed, at low laser beam velocities, the morphology is higher and quality of track presents many defects than at high laser beam velocities.

This study involved LSR treatment of hypoeutectic Al-2.0

wt.% Fe alloy. The samples was characterized by various techniques, including optical microscopy (OM), scanning electron microscopy (SEM) and vickers microhardness test. Analysis of Vickers hardness were done in the cross-sectional area of treated sample and on the treated sample surface. The microstructure and microhardness of laser-treated layer were systematically investigated to correlate their properties with process involved.

Materials and Methods

Material

Hypereutectic Al-2.0 wt.% Fe alloy under study was prepared with commercially pure raw materials. The material was cast in a resistance furnace (muffle) by pouring the liquid metal into a cylindrical ingot mold and cooling in ascending mode. Resulting ingot was sectioned into various samples, which were sand blasted individually to determine the chemical composition of alloy by energy-dispersive X-ray fluorescence spectrometry (Shimadzu EDX-7000), as indicated in Table 1.

Table 1. Chemical composition of materials used for manufacture of Al-2.0 wt.%Fe alloy.

Material	Impurity			
	Fe	Si	Cu	Ni
Al 99.76%	0.09%	0.06%	0.06%	0.03%
Fe 99.97%	-	0.01%	0.01%	0.01%

Laser surface treatment

In this research, Al-2.0wt% Fe alloy was applied to a laser surface remelting (LSR) process, without gas protection, using a 2 kW Yb-fiber laser (IPG YLR-2000S) in order to examine treated and untreated layers. LSR treatment was performed in a laboratory at Institute for Advanced Studies (IEAv) of Aerospace Technical Center (CTA–ITA) in São Jose dos Campos, SP, Brazil. A laser scanning speed of 40 mm s−1 was applied. Average power of the laser beam was set at 600 W and the power density on the sample surface was estimated at 4.8 ×105W cm−2. Laser-treated samples were covered with several weld fillets during the remelting process [5].

Equipment for microstructural and morphological characterization

Various microstructural characterization techniques were employed to gain a better understanding of microstructural effects of Al–2.0 wt.%Fe alloy LSR-treated under this study. Th techniques applied procedure were optical microscopy (OM), field-emission scanning electron microscopy (FES-EM) coupled to energy dispersive spectroscopy (EDS) and Vickers microhardness testing, which are described in details below.

LSR treated samples were analyzed by OM (Olympus BX51) couple to a Q-Color 3 digital camera to capture images. Prior to studying the LSR treated layer, the cross-sections were cut out of the samples using a diamond blade and they were sanded and polished. Samples were chemically etched with hydrofluoric acid 0.5 % (v/v) at intervals 30 to 45 seconds, after they were polished with metallographic polishing pads, using only water, to ensure that LSR treatment would not be impaired.

Laser-treated material and substrate were analyzed by FES-EM (MIRA 3 LM) coupled to EDS to examine the microstructural changes caused by laser treatment.

Vickers microhardness testing

Vickers hardness (HV) tests were performed using a Leica VMHT MOT microhardness tester operating with a load of 0.1 kg at 15 seconds (HV 0.1 15s). The tester was applied in the cross-sectional area of treated specimen, to different penetration depths until it reached the base material. Penetration depths of the tester from the surface in the treated material region were approximately 50µm, 100µm and 200µm, however, 300µm, 500µm and 700µm were in the base material region as shown on schematic in Figure 1. At each of these depths, 15 micro-indentations were made in lines parallel to surface. Average hardness and standard deviation at each of selected depths were calculated based on data obtained.

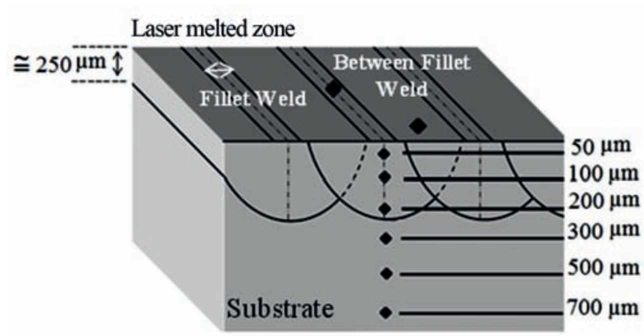

Figure 1 – Schematic diagram of weld fillets on the sample surface and in the cross-sectional area showing the penetration depth of Vickers indenter in LSR-treated sample

For preparation of HV tests, a cross-sectional sample was sanded with 600 and 1200 grit sandpaper and polished with colloidal silica to reduce its roughness, thereby preventing roughness that could interfere in the results of HV measurements. Besides, microhardness was measured on the laser-treated sample surface, which was cleaned only with water to prevent that it could be modified. Furthermore, the material's hardness was tested on the weld fillets region and between them.

Results and Discussion

Surface characterization of laser-treated samples

Figure 2 illustrates the morphology of hypereutectic Al-2.0 wt.% Fe alloy laser-treated and analyzed by OM and FES-EM, showing characteristics of the weld fillets formed du-

Edición digital

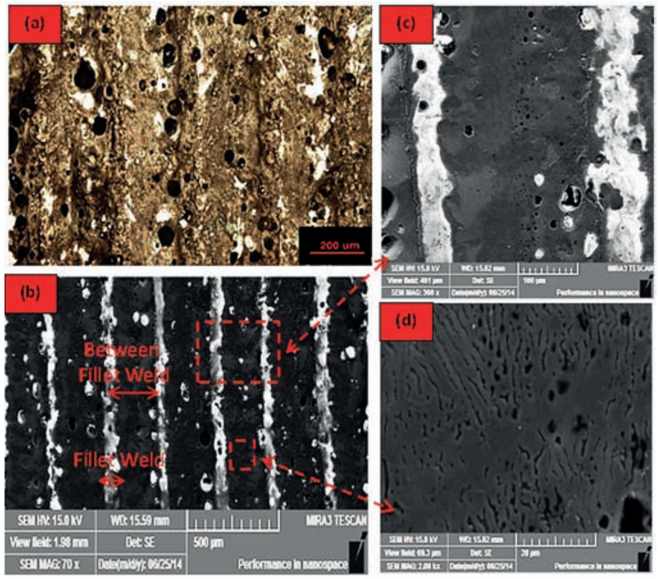

Figure 2 – (a) OM, and (b) FESEM images of the morphology of hypereutectic Al-2.0 wt% Fe alloy LSR-treated surface, showing regions on the weld fillet and between the weld fillets, (c) on the weld fillet region at increase magnification, and (d) between weld fillets region under higher magnification.

ring laser treatment. OM image in Figure 2(a) shows the surface morphology, while FESEM image in Figure 2(b) shows the morphology in more detail on the weld fillets region and between the weld fillets. As can be seen, on the weld fillet region contains a higher concentration of defects if compared with the weld fillets region. Zhang et al. [6] and Kalita et al. [1] reported a similar result. In Figure 2(b), the distance between the weld fillets is approximately 300 μm. It was notecid the presence of several nanopores, which may be attributed to volatilization of inclusions or vaporization of the substrate itself, caused by hydrogen and moisture in the atmospheric air, which are absorbed in the laser-treated region favoring the formation of pores. These results are consistent with reported of Yilbas et al. [7] and Pariona et al. [2]. The micrograph in Figure 2(c) shows on the weld fillets region under higher magnification, it showing concentration of defects in more details. Figure 2(d), also at increased magnification, shows between the weld fillets region, a more uniform morphology with a columnar-like structure. Pariona et al. [2] also observed these structures in Al-1.5 wt% Fe and Li et al. [8], these last authors stated that Al-Co-Ce alloys contain Al-rich eutectic regions whose structure and was similar to Al-2.0wt.% Fe alloy. Peculiar characteristics of the microstructure shown in Figure 2 (d), resented by a highly improved properties, such as: hardness, corrosion and wear resistance, which is resulted of precipitates dissolution and formation of metastable phases. Several authors have reported similar results, among them, Damborenea [9], Pinto [10], Yue et al. [11], Majumdar et al. [12], Bertelli et al. [13], and Pariona et al. [2].

Pariona et al. [2] analyzed hypoeutectic Al-1.5 wt.% Fe alloy LSR-treated and observed presence of microcracks between the weld fillets. However, this phenomenon in this study was not observed in hypereutectic Al-2.0 wt% Fe alloy LSR-treated, as can be seen in Figure 2(c) and (d). Lack of microcrack was expected, since, according to Mondolfo [14], formation Al-Fe alloys is impaired, when the material contains coarse Al3Fe particles or intermetallic phase, which tend to producemicrocracks and reduce formability, whereas, this does not occur with presence of Al6Fe finely dispersed in Al-2.0 wt.% Fe alloy, however, the Al3Fe intermetallic phase does not appear in this alloy, as demonstrated by Pariona and Micene [15] by low-angle X-Ray diffraction analysis. Meanwhile, Gremaud et al. [16] reported, increasing the cooling rate of hypereutectic alloys containing up to 9 wt.% of Fe suppresses formation of stable Al3Fe phase, which is replaced by Al6Fe phase, which confirms our result.

Characterization in the cross-section of laser-treated and untreated materials

Figure 3 shows a cross-sectional analysis by OM. In this region can be observed the penetration depth of the treated region was around 250 μm, and the distance between the weld fillets was approximately 300 μm (also was shown in the first micrograph, Figure 2). Note clearly visible difference of the treated region microstructure and of the substrate.

The laser melted surface micrograph is shown at Figure 3, as can be seen it is free of microcracks and the melted regions are free of precipitates too. A fine microstructure of the melt zone is attributed to high cooling rate. Microstructure obtained in this work is similar to other laser melted aluminum alloys, as reported in the literature, i.e., Watkins et al. [17] reported that the microstructure of laser melted AA 2014 consists of columnar grains growing epitaxially from the substrate. Although, maximum melt depth observed in this work was 250μm (Fig. 3); however the thickness of this zone depends of laser power and of the Maragoni effect, as was discussed by Pariona et al. [5], these authors demonstra-

Edición digital

ted when the laser beam velocity is low, therefore the molten zone depth is greater.

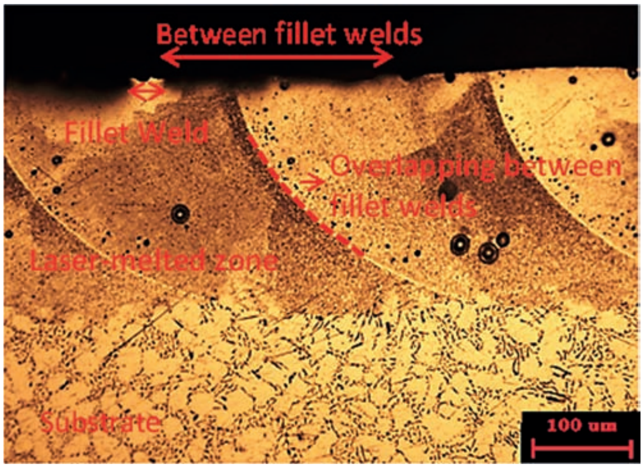

Figure 3 – OM micrograph in the cross sectional area of laser-treated material

Figure 3 also shows zones where there is overlapping of consecutive weld fillets. This overlapping is more common in Al-2.0 wt.% Fe alloy than in Al-1.5 wt.% Fe alloy, reported by Pariona et al. [2, 3, 5]. Kalita et al. [1] also reported overlapping of consecutive weld fillets and Cordovilla et al. [17] pointed out as essential tool to understand way in which each track affects the microstructures produced by previous one

Figure 4 depicts a cross-sectional LSR-treated sample and analyzed by SEM, showing some regions of substrate and the as-cast microstructure. In the cast area in Figure 4, note presence of protuberances, which correspond to on the weld fillet region (also shown in Figure 3). According to Pariona et al. [4], presence of protuberances is more noticeable in Al-1.5 wt.% Fe alloy than in Al-2.0 wt.% Fe alloy. Figure 4(a) also shows an overlapping line of consecutive weld fillets. Figure 4(b) and (e) show the substrate region and the laser-treated area under higher magnification, showing a visibly different microstructure, with a dendritic-like structure. This microstructural difference between untreated substrate and LSR-treated region is attributed to temperature applied on the material surface, which exceeded its melting point but was lower than boiling point, followed by rapid cooling in laser treatment process and this leads a high thermal gradient, and so in this way produces the laser melted zone. This treatment resulted in formation of a thin recast layer with a refined microstructure practically free of precipitates, inclusions and intermetallic phases [16], as can be clearly seen at the magnified image, Figure 4(d), with a columnar dendrite structure, Watkins et al. [17] and, Grum and Sturm [18] have also reported this characteristic in laser cast materials. Figure 4(c) shows the substrate region, which is also displayed under higher magnification in Figure 4(f), showing presence of intermetallic phase dispersed in the matrix. A comparison in more detail of Figures 4(d) and 4(f) reveals that the treated region morphology is more homogeneous, without presence of the intermetallic phase that extends throughout the recast area and showing evidence of transition from coarse-grained to fine-columnar-dendrite structure. According to Pariona et al. [2], behavior of the laser treated region is homogeneous and similar to an amorphous phase; hence, it shows greater hardness, lower surface roughness, and higher corrosion resistance, reported by Pariona and Micene [15].

Vickers Microhardness Test

Vickers hardness test was accomplished in this work and by means of a microscope coupled to the tester, the “d1” and “d2” diagonals formed in area indented by pyramid were measured, and these parameters were used to calculate Vickers hardness. Figure 5 illustrates indented areas used for

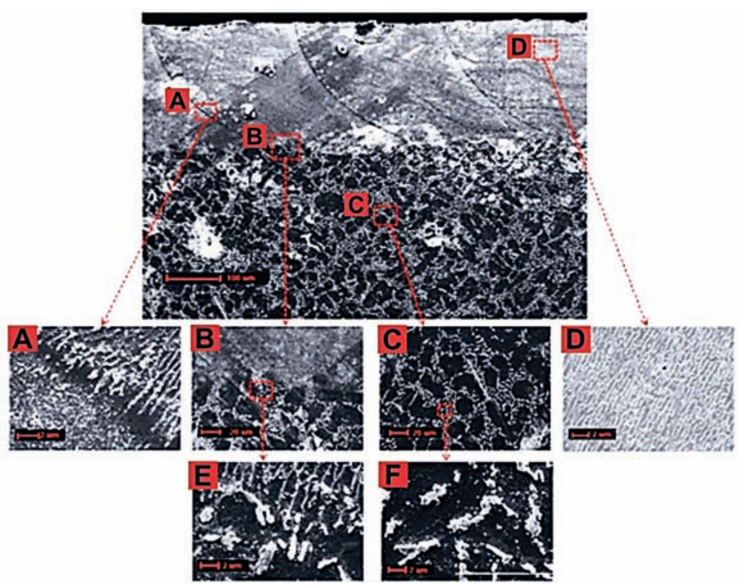

Figure 4 – SEM micrograph in the cross-sectional sample of Al-2.0 wt.% Fe alloy LSR-treated: (a) overlapping line of consecutive weld fillets, (b) interface of treated surface and substrate, (c) substrate unaffected by laser treatment, (d) detail in the cast region, (e) interfacial region of the treated surface and substrate, and (f) detail of the substrate unaffected by laser treatment.

calculation of the hardness of Al-2.0 wt.% Fe samples.

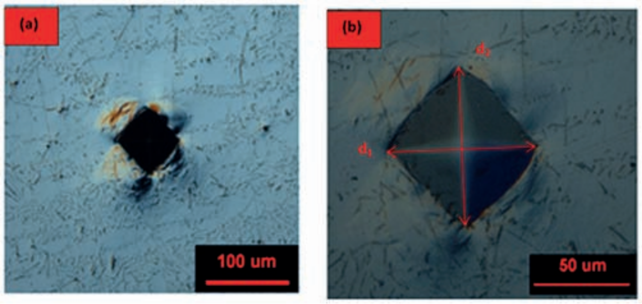

Figure 5 – (a) Area indented by HV tester in Al-2.0 wt.% Fe sample, (b) deformed region shown under higher magnification

Microhardness profiles were measured along in a cross-sectional sample, for laser-treated layer and untreated. These measurements were taken along lines parallel to surface at depths of 50, 100, 200, 300, 500 and 700 µm, applying a load of HV 0.1 for 15s. Figure 6 illustrates, the 15 micro-indentations made in the cross section and at each of these depths to measure the hardness. Average hardness values and standard deviation (s.d.) at each depth were calculated based on these measurements, and are given in Table 2.

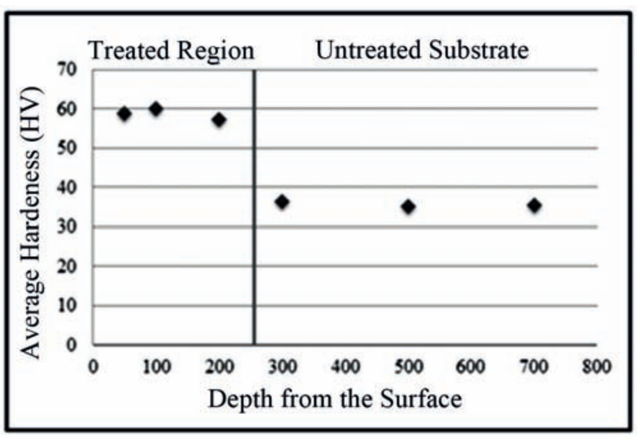

Figure 6 – Vickers hardness analysis (HV 0.1 15s) of LSR-treated layer and untreated substrate.

Table 2. Vickers hardness Analysis in a cross-sectional area, in sample treated and untreated (VH 0.1 15s).

Region	Depth the surface	Average of VH	S.d Deviation of VH
Treated region	50 µm	59.0	3.15
	100 µm	60.0	3.8
	200 µm	57.4	3.0
Untreated region	300 µm	36.5	1.43
	500 µm	35.2	1.44
	700 µm	35.4	1.68

An analysis of the data in Table 2 indicates the HV is the higher on the LSR treated region than the untreated region. The average hardness of the treated region is 58.8 HV, while that of the untreated region is 35.7 HV, which corresponds at 60.7% increase in hardness in the treated region compared to the untreated region.

The data in Table 2, also is shown in graphical form in Figure 7, it clearly show increase in hardness at treated region than untreated substrate. This difference is attributed to microstructural changes as resulting of LSR-treated. In other studies involving LSR treatment of materials, similar results have been obtained by Yao et al. [19] and others, who reported a significant increase in hardness in laser-treated region than untreated region.

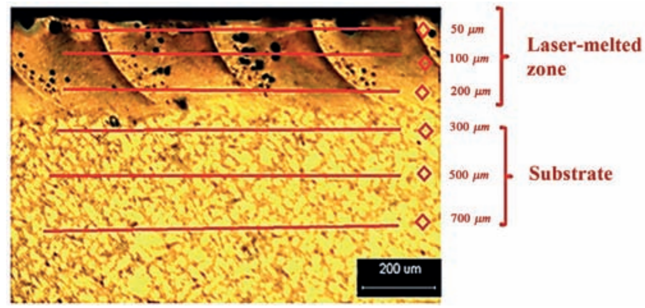

Figure 7 – OM image in the cross section of Al-Fe sample laser-treated, indicating the depths selected for microhardness measurements.

The material surface hardness was also analyzed by HV measurements on the weld fillets region and between them (see Figures 2, 3 and 4), for the as-received laser-treated sample. The average Vickers hardness was calculated for 15 micro-indentations made on the weld fillets and between the weld fillets, as indicated in Table 3.

Table 3. Analysis of Vickers hardness on the treated sample surface, indicating the hardness at the regions on the weld fillets and between the weld fillets (VH 0.1 15s).

Region	Average of VH	Standard Deviation of VH
On the weld fillets	52.68	6.18
Between the weld fillets fillets	59.14	5.53

As can be seen in Table 3, the HV values measured on the sample surface are consistent with those measured in the cross-section too, so showing a higher average hardness at the region between the weld fillets than on the weld fillet. Pariona et al. [3], who made a comparative analysis of the HV of Al-1.5 wt.% Fe alloy measured on the weld fillets and between the weld fillets, also reported that the hardness between the weld fillets was higher than on the weld fillets, therefore, the surface hardness in the laser-treated region in relation to the untreated region is high, due to the treated region morphology is more homogeneous, without presence of intermetallic phase (Al_3Fe) and with the presence of Al_6Fe phase finely dispersed in the matrix that extends throughout the recast area, as can be checked in Figures 2, 3 and 4.

Present study focused on the microstructural characterization of hypereutectic Al-2.0 wt.% Fe alloy, while previous studies by Pariona et al. [2-4] involved hypoeutectic Al-1.5 wt.% Fe alloy. Although both alloys were castings and solidified by laser-treated process in the same conditions, however, microstructural analysis of the two alloys revealed characteristics different. The overlapping line of consecutive weld fillets at the cast zone of Al-1.5 wt.% Fe alloy was barely perceptible than Al-2.0 wt.% Fe alloy. In addition, also in the cast zone, presence of protuberances on the weld fillets was much more noticeable at Al-1.5 wt.% Fe alloy than at Al-2.0 wt.% Fe alloy. However, Al-1.5 wt.% Fe alloy showed a behavior lamellar at the cast zone and meanwhile Al-2.0 wt.% Fe alloy showed a behavior fine-columnar-like structure. Both alloys showed nanopores, which were concentrated mostly on the weld fillets. The microhardness of Al-2.0 wt.% Fe alloy LSR-treated surface was slightly more higher than Al-1.5 wt.% Fe alloy.

This alloy has an industrial applications potential in the automotive, aerospace, electronics, and other sectors. This type of study has shown interesting and innovative results.

Conclusions

This research involved a study of hypoeutectic Al-2.0 wt.% Fe alloy subjected to a laser surface remelting (LSR) treatment. The main results are the following:

1. In the cast region shown a refined compact and homogeneous microstructure devoid of microcracks and with formation of a small protuberance,
2. The treated region showing evidence of transition from coarse-grained to fine-columnar-like structure,
3. Fine microstructure of the melt zone is attributed to high cooling rate due to LSR-treated,
4. The cast region of Al-2.0 wt.% Fe alloy showed a noticeable overlapping line of consecutive weld fillets,
5. The hardness of the cast region of Al-2.0 wt.% Fe alloy was about 61% higher than the untreated material,
6. A higher average hardness at the between the weld fillets region than on the weld fillet was shown,
7. This alloy is potentially applicable in the automotive, aerospace and electronics sectors, due to its high hardness and the morphology of laser-treated alloy presented a fine-columnar-like structure than the untreated material.

Acknowledgements

This work was entirely financed by CNPq (Brazilian National Council for Scientific and Technological Development), Fundacao Araucaria (FA), CAPES (Federal Agency for the Support and Evaluation of Postgraduate Education), and FINEP (Research and Projects Financing Agency). We also thank to LABMU-UEPG.

References

[1] S.J. Kalita, *Microstructure and corrosion properties of diode laser melted friction stir weld of aluminum alloy 2024 T351*, Applied Surface Science 257(9) (2011) 3985–3997.

[2] M.M. Pariona, V. Teleginski, K. Santos, S. Machado S, A.J. Zara, N.K. Zurba, R. Riva. *Yb-fiber laser beam effects on the surface modification of Al–Fe aerospace alloy obtaining fillet weld structures, low fine porosity and corrosion resistance*, Surface and Coatings Technology 206 (2012 I) 2293–2301.

[3] M.M. Pariona, V. Teleginski, K. dos Santos, E.L.R. dos Santos, A.A.O.C. de Lima, R. Riva, *AFM study of the effects of laser surface remelting on the morphology of Al Fe aerospace alloys*, Materials Characterization 74 (2012 II) 64-76.

[4] M.M. Pariona, A.F. Taques, L.A. Woiciechowski, *The Marangoni effect on microstructure properties and morphology of laser-treated Al-Fe alloy with single track by FEM: Varying the laser beam velocity*, International Journal of Heat and Mass Transfer 119 (2018) 10-19.

[5] M.M. Pariona, V. Teleginski, K. dos Santos, A.A.O.C. de Lima AAOC, A.J. Zara, T.M. Micene, R. Riva, *Influence of laser surface treated on the characterization and corrosion behavior of Al–Fe aerospace alloys*, Applied Surface Science 276 (2013) 76– 85.

[6] X. Zhang, J. She, S. Li, S. Duan, Y. Zhou, X. Yu, R. Zheng, B. Zhang, *Simulation on deforming progress and stress evolution during laser shock forming with finite element method*, Journal of Materials Processing Technology 220 (2015) 27–35.

[7] B.S. Yilbas and N. Al-Aqeeli, *Analytical investigation into laser pulse heating and thermal stresses*, Optics & Laser Technology 41 (2009) 132–139.

[8] R. Li, M.G.S. Ferreira, A. Almeida, R. Vilar, K.G. Watkins, M.A. McMahon, W.M. Steen, *Localized corrosion of laser surface melted 2024-T351 aluminum alloy*, Surface and Coatings Technology, 81: 290-296.

[9] Damborenea J (1998) *Surface modification of metals by high power lasers*, Surface and Coatings Technology100-101 (1996) 377-382.

[10] M.AQ. Pinto, N. Cheung, M.C.F. Ierardi MCF, A. Garcia, *Microstructural and hardness investigation of an aluminum-cooper alloy processed by laser surface melting*, Materials Characterization 50 (2003) 249-253.

[11] T.M.Yue, L.J. Yan, C.P. Chan, C.F. Dong, H.C. Man, G.K.H. Pang GKH, *Excimer laser surface treatment of aluminum alloy AA7075 to improve corrosion resistance*, Surface and Coatings Technology 179 (2004) 158-164.

[12] J.D. Majumdar, A. Pinkerton. Z. Liu Z, I. Manna, L. Li, *Microstructure characterization and process optimization of laser assisted rapid fabrication of 316L stainless steel*, Applied Surface Science 247 (2005) 320-327.

[13] F. Bertelli, E.S. Meza, P.R. Goulart, N. Cheung, R. Riva, A. Garcia, *Laser remelting of Al–1.5wt.% Fe alloy surfaces: numerical and experimental analyses*, Optics and Lasers in Engineering 49 (2011) 490-497.

[14] L.F. Mondolfo, *Aluminum alloys: Structure and properties*. 9. ed. London, Butterworths, 1976.

[15] M.M. Pariona and K.T. Micene, *The alumina film nanomorphology formed to improve the corrosion resistance of Al–2.0 wt.%Fe alloy as result of the laser surface melting technique applied*, Advances in Chemical Engineering and Science 7 (2017) 10-22.

[16] M. Gremaud, M. Carrard, W. KURZ, *The microstructure of rapidly solidified Al-Fe alloys subjected to laser surface treatment*, Acta Metallurgia et Materialia 38 (1990) 2587-2599.

[17] K.G. Watkins, Z. Liu, M. McMahon, R. Vilar, M.G.S. Ferreira, 1998 *Influence of the overlapped area on the corrosion behaviour of laser treated aluminium alloys*, Materials Science and Engineering A 252 (1998) 292–300.

[18] J. Grum, R. Sturm, *A new experimental technique for measuring strain and residual stresses during a laser remelting process*, Journal of Materials Processing Technology 147 (2004) 351-358.

[19] Y. Yao, X. Li, Y.Y. Wang, W. Zhao, G. Li, R.P. Liu, *Microstructural evolution and mechanical properties of Ti–Zr beta titanium alloy after laser surface remelting*, Journal of Alloys and Compounds 583 (2014) 43-47.